

## Magnetic anisotropy in Ni/Fe and Fe/Cu/NiFe multilayers

This article has been downloaded from IOPscience. Please scroll down to see the full text article.

1999 J. Phys.: Condens. Matter 11 3449

(<http://iopscience.iop.org/0953-8984/11/17/304>)

View [the table of contents for this issue](#), or go to the [journal homepage](#) for more

Download details:

IP Address: 171.66.16.214

The article was downloaded on 15/05/2010 at 07:20

Please note that [terms and conditions apply](#).

## Magnetic anisotropy in Ni/Fe and Fe/Cu/NiFe multilayers

J A Hutchings<sup>†</sup>, K Newstead<sup>†</sup>, M F Thomas<sup>†</sup>, G Sinclair<sup>‡</sup>, D E Joyce<sup>‡</sup> and P J Grundy<sup>‡</sup>

<sup>†</sup> Department of Physics, University of Liverpool, Liverpool L69 7ZE, UK

<sup>‡</sup> Department of Physics, University of Salford, Salford M5 4WT, UK

Received 14 September 1998, in final form 25 February 1999

**Abstract.** Multilayer samples of Ni/Fe and Fe/Cu/NiFe, fabricated by sputtering and characterized by transmission electron microscopy and electron diffraction, were studied by <sup>57</sup>Fe Mössbauer spectra and magnetization measurements. Mössbauer spectra taken in zero applied field at 300 K and 4.2 K showed midlayer and interface iron sites in Ni(20 Å)/Fe(*x* Å) samples with *x* = 20 Å, 30 Å, 50 Å, 80 Å and in-plane spin orientation. The reorientation of the magnetic moments at 4.2 K in increasing fields applied normal to the layers when combined with magnetization measurements enabled the magnetic anisotropy energy *K* of each sample to be evaluated. The trend of the values of *K* with iron layer thickness gave volume and interface anisotropy components  $K_V = (-5 \pm 1) \times 10^4 \text{ J m}^{-3}$  and  $K_S = (-0.6 \pm 0.4) \times 10^{-3} \text{ J m}^{-2}$  where negative values indicate in-plane preference. Similar measurements on a series of samples of Fe(30 Å)/Cu(*x* Å)/Ni(80%)Fe(20%)(30 Å) with *x* = 10 Å, 20 Å, 30 Å, 50 Å showed a tendency toward increasing in-plane anisotropy energy *K* with decreasing thickness of the non-magnetic Cu layer.

### 1. Introduction

Over the past ten years the magnetic properties of metallic multilayer systems incorporating magnetic layers have been intensively studied. The characterization of the crystal structure nature of the layers and interfaces has been probed. The dependences of the interactions between the magnetic layers on the material, crystal structure and thicknesses of the magnetic and non-magnetic layers have been investigated in an attempt to understand the mechanisms and produce composite materials with desirable properties. Details of the extensive work on a variety of multilayer systems are reported in several reviews [1–3]. A property of particular interest in these systems is the magnetic anisotropy energy—the energy difference between the ferromagnetic moment alignment in plane and out of plane. This interest in the anisotropy arises from the possible use of magnetic multilayers in magneto-optical recording where magnetic moment alignment normal to the layers is favoured.

The geometry of the magnetic layer however leads to a shape-dependent demagnetizing energy  $-\frac{1}{2}\mu_0 M^2$  per unit volume acting to keep the magnetic moments in plane. For out-of-plane spin alignment to be achieved, anisotropy terms of sufficient magnitude and favouring normal spin orientation must arise. For some very thin magnetic layers, interface and surface anisotropies provide such terms. Reviews have been written which focus on this property of magnetic anisotropy in multilayers [4–6]. The present work aims to study two different aspects of the anisotropy energy in selected multilayer systems. The first is to measure the intrinsic anisotropy *K* (the anisotropy excluding the  $-\frac{1}{2}\mu_0 M^2$  demagnetizing term) of the Ni/Fe interface in a situation where the overall anisotropy is dominated by the demagnetizing

energy. The second is to investigate whether any change in magnetic anisotropy energy  $K$  occurs when the interaction between separated magnetic layers is increased by reducing the thickness of an intervening non-magnetic layer.

## 2. Experimental technique

Multilayer samples were fabricated by magnetron sputtering using an Atomtech 2000 system at the University of Salford. The system has a base pressure of  $10^{-7}$  mbar and the sputtering is conducted at a pressure of 3 mbar of Ar. Multilayers were grown on substrates of an iron-free polyester (Mylar) of thickness 0.05 mm which was kept at room temperature during the deposition of the layers. Deposition rates of  $0.71 \text{ \AA s}^{-1}$ ,  $1.69 \text{ \AA s}^{-1}$  and  $1.37 \text{ \AA s}^{-1}$  for iron, copper and permalloy were determined using x-ray fluorescence. Two series of samples were fabricated:

- (a)  $[\text{Ni}(20 \text{ \AA})/\text{Fe}(x \text{ \AA})]_n$  where  $x = 20 \text{ \AA}$ ,  $30 \text{ \AA}$ ,  $50 \text{ \AA}$  and  $80 \text{ \AA}$  and  $n = 100, 65, 40$  and  $25$ . The values of  $n$  were determined by the requirement of  $\sim 2000 \text{ \AA}$  of natural iron (2.2%  $^{57}\text{Fe}$ ) per sample to obtain an adequate Mössbauer signal.
- (b)  $[\text{Fe}(30 \text{ \AA})/\text{Cu}(x \text{ \AA})/\text{NiFe}(30 \text{ \AA})]_{50}$  with  $x = 10 \text{ \AA}$ ,  $20 \text{ \AA}$ ,  $30 \text{ \AA}$  and  $50 \text{ \AA}$ .

The NiFe (permalloy) layers have a composition of 80% Ni, 20% Fe. These samples can thus be envisaged as magnetic bilayers of Fe(30 Å) and NiFe(30 Å) separated by non-magnetic copper layers. Mössbauer spectra were taken in the conventional transmission mode requiring substrates transparent to the  $^{57}\text{Fe}$  14.4 keV Mössbauer gamma rays. This mode was chosen in order to take spectra in applied fields at 4.2 K. Sources of  $^{57}\text{Co}$  in a Rh matrix of strengths up to 100 mCi were used. The multilayers were too thin to obtain an optimum signal/noise ratio and Mössbauer samples were made by assembling up to five layers of the multilayer in a polypropylene holder. Such samples were still at the thin-sample limit and, with counting rates of  $5 \text{ K s}^{-1}$  to  $10 \text{ K s}^{-1}$ , several days were required to achieve an acceptable spectrum. The spectrometers were run with a waveform giving alternate positive and negative velocity-versus-time slopes and the spectra folded so that the background was flat. The spectrometers were calibrated using  $25 \text{ \mu m}$  foils of  $\alpha$ -iron run at room temperature and isomer shift values are quoted relative to this standard. External fields were applied at 4.2 K by a superconducting magnet in which the field was applied normal to the plane of the multilayer absorber and the gamma ray beam was parallel to the field direction.

Measurements of the magnetization  $M$  were made on the Aerosonic 2001 vibrating-sample magnetometer (VSM) in the Department of Physics at the University of Manchester. The magnetometer was calibrated with a standard nickel foil and hysteresis cycles were taken at room temperature in fields in the range  $-5 \text{ T} \leq B \leq +5 \text{ T}$  with the field applied in the plane of the layers.

## 3. Characterization and results

### 3.1. Ni/Fe multilayer characterization

The samples Ni(20 Å)/Fe( $x$  Å),  $x = 20 \text{ \AA}$ ,  $30 \text{ \AA}$ ,  $50 \text{ \AA}$  and  $80 \text{ \AA}$ , henceforth denoted as 20/20, 20/30, 20/50 and 20/80, were fabricated by magnetron sputtering with layer thicknesses determined by timing the calibrated deposition rates. The layer structure was observed by observing, with transmission electron microscopy, a sliced cross section through the multilayer. The thin cross sectional slices were taken with an LKB 8800 Ultratome microtome and the slices were observed with the JEOL 3010 electron microscope in the Physics Department at the

University of Salford. The layering images observed gave layer thicknesses consistent with those obtained from deposition rates. Attempts to monitor the layer thickness with low-angle x-ray diffraction were unsuccessful due to the lack of flatness of these layers deposited on Mylar substrates.

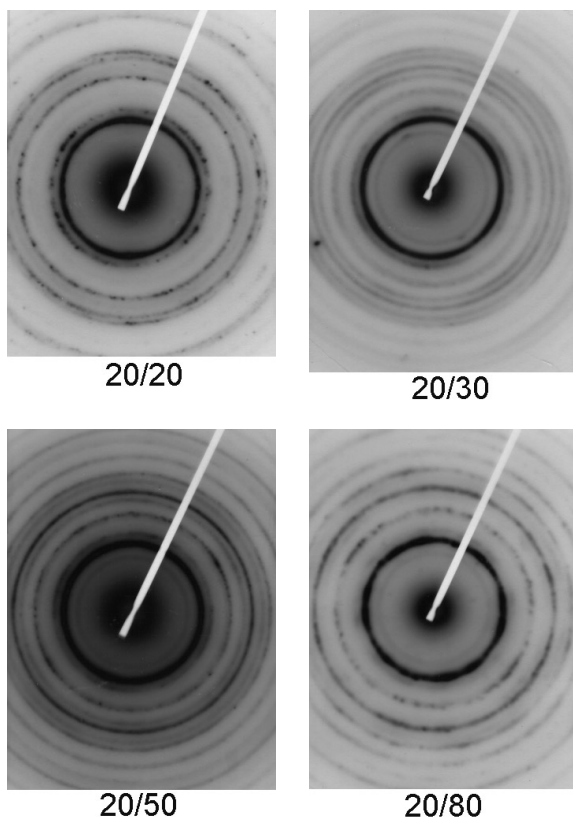


**Figure 1.** Electron diffraction rings from Ni/Fe multilayer samples taken with a JEOL 3010 electron microscope. The 20/20 sample shows rings with lattice spacings characteristic of fcc nickel. For the 20/30, 20/50 and 20/80 samples, extra rings with lattice spacings characteristic of bcc iron are observed.

The crystal structure of the layers was studied by electron diffraction using the JEOL 3010 electron microscope. Diffraction rings from the 20/20, 20/30, 20/50 and 20/80 samples are shown in figure 1. For the 20/20 sample, rings are identified with interplane spacings of  $2.03 \pm 0.02 \text{ \AA}$ ,  $1.74 \pm 0.02 \text{ \AA}$ ,  $1.23 \pm 0.02 \text{ \AA}$  and  $1.05 \pm 0.02 \text{ \AA}$  characteristic of the fcc Ni planes (111), (200), (220) and (311) respectively. The iron bcc phase has interplane spacings of  $2.03 \text{ \AA}$ ,  $1.43 \text{ \AA}$ ,  $1.17 \text{ \AA}$  and  $1.01 \text{ \AA}$  from (110), (200), (211) and (220) planes. While the Fe(110) ring would coincide with the Ni(111) ring, no evidence is seen for other Fe bcc rings. Thus while electron diffraction provides no evidence for Fe bcc structure in the 20/20 sample, it is possible that some signal from this phase could exist. For the samples 20/30, 20/50 and 20/80, electron rings are observed at interplane spacings of  $1.41 \pm 0.02 \text{ \AA}$ ,  $1.14 \pm 0.02 \text{ \AA}$  and  $1.00 \pm 0.02 \text{ \AA}$ , characteristic of bcc iron, in addition to the rings characteristic of the fcc nickel. The intensities of the bcc rings are seen to increase as expected with increasing iron layer thickness.

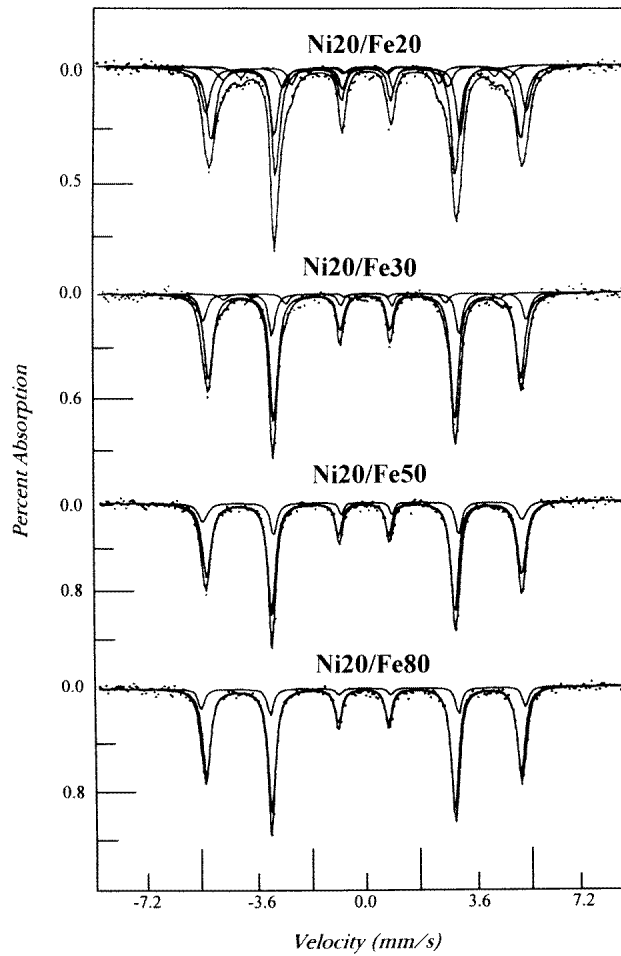


**Figure 2.** Mössbauer spectra taken at 300 K for Ni/Fe multilayers. The spectra refer, in descending order, to the 20/20, 20/30, 20/50 and 20/80 samples. The spectra are fitted with magnetic sextet components each corresponding to a distinct iron-atom environment. In each spectrum the individual components are shown in addition to the overall summed fit. The parameters of the fitted components are listed in table 1.

The samples were further characterized by means of the Mössbauer spectra taken at 300 K and shown in figure 2. These spectra were taken with high statistics to identify in detail the iron environments within the samples. The fitting parameters of the components and their relative areas are listed in table 1. The spectra were fitted with several magnetic sextet components each corresponding to a distinct iron-atom environment. The component with isomer shift  $\delta = 0.01 \pm 0.01 \text{ mm s}^{-1}$ , quadrupole interaction  $\Delta = +0.02 \pm 0.01 \text{ mm s}^{-1}$  and hyperfine field  $B_{hf} = 330 \pm 1 \text{ kG}$  is observed to be the main component for all samples and to increase in relative area as the iron layer thickness increases. This component is identified with bcc iron in agreement with several studies [7–9] which show that iron layers with thicknesses greater than  $\sim 40 \text{ \AA}$  have bcc structure. The component next in intensity has isomer shift  $\delta = 0.03 \pm 0.02 \text{ mm s}^{-1}$ , a mean quadrupole interaction  $\Delta = -0.05 \pm 0.02 \text{ mm s}^{-1}$  and hyperfine field  $B_{hf} = 340 \pm 5 \text{ kG}$ . In NiFe alloys such parameters characterize Fe-

**Table 1.** Hyperfine fitting parameters for the Mössbauer spectra of the Ni/Fe multilayers taken at 300 K and shown in figure 2. For the main component the errors on the isomer shift, quadrupole interaction, hyperfine field and relative area are  $\pm 0.01 \text{ mm s}^{-1}$ ,  $\pm 0.01 \text{ mm s}^{-1}$ ,  $\pm 1 \text{ kG}$  and  $\pm 4\%$  respectively. For the other components the errors are approximately double these values.

Multilayer Ni/Fe	Component	Isomer shift ( $\text{mm s}^{-1}$ )	Quadrupole interaction ( $\text{mm s}^{-1}$ )	Hyperfine field (kG)	Relative area (%)
20/20	1	0.01	0.02	328	50
	2	0.03	-0.04	340	32
	3	0.02	0.08	270	8
	4	-0.02	0.02	303	10
20/30	1	0.01	0.01	329	74
	2	0.03	-0.02	341	21
	3	-0.03	-0.13	291	5
20/50	1	0.01	0.04	331	80
	2	0.03	-0.11	336	20
20/80	1	0.01	0.02	330	85
	2	0.03	-0.03	340	15

rich alloys with bcc structure [10]. The non-zero quadrupole interaction for this interface site is comparable to that observed in Fe monolayers at clean Fe surfaces and Fe/Ag interfaces [11]. The components of lesser intensity, seen only in 20/20 and 20/30 samples, are characterized by hyperfine fields below the Fe bcc value of 330 kG and are consistent with parameters of Ni-rich NiFe alloys with fcc structure [10] in the iron layers. Thus the Mössbauer results can be interpreted as giving bcc/fcc intensity ratios for the iron layers of 82/18, 95/5, 100/0 and 100/0 for the 20 Å, 30 Å, 50 Å and 80 Å layers respectively.

A number of studies have been made on Fe layers grown on Ni substrates or in Ni/Fe multilayers [7–9, 11–16]. It appears that details of the Fe structure can depend on the thickness of the Ni substrate or surrounding layers, and the method and rate of deposition. However, a common feature is the observation of the growth of an fcc or fct (face-centred tetragonal) structure if the iron layer has thickness  $t \leq 20 \text{ Å}$ . Layers with  $t \geq 20 \text{ Å}$  are usually observed to have the bcc structure.

In the most detailed study of Ni/Fe multilayers produced by sputtering and with layer thicknesses similar to those of our samples [8], iron layers with  $t \leq 7 \text{ Å}$  were observed to form an fct structure with close to bulk magnetic magnetization, while for  $7 \text{ Å} \leq t \leq 14 \text{ Å}$  an fcc phase was seen with low magnetization. For layers with  $t \geq 15 \text{ Å}$  a bcc structure was observed. This is consistent with our attribution of predominantly bcc structure for our iron layers with  $t \geq 30 \text{ Å}$ . A final test addresses the possibility that the Mössbauer component of 330 kG—particularly in the  $t = 20 \text{ Å}$  iron layers—could represent an fcc antiferromagnetic phase having hyperfine field close to that for the  $\alpha$ -bcc phase. Such a phase has been reported in iron layers grown on Cu(001) though with an isomer shift  $\delta \sim 0.15 \text{ mm s}^{-1}$  which is inconsistent with our measured value [17]. Accordingly the magnetizations of the samples were measured for the 20/20, 20/30, 20/50 and 20/80 multilayers using a vibrating-sample magnetometer. The values of saturation magnetization obtained, listed in table 2, confirm that the magnetizations of all of the Fe layers are consistent with their bulk bcc values and incidentally that in all of the multilayers the iron and nickel layers couple ferromagnetically.

**Table 2.** Values of the magnetization  $M$ , demagnetizing energy  $-\frac{1}{2}\mu_0 M^2$  and intrinsic anisotropy energy  $K$  for the multilayer systems listed. The errors in  $M$  and  $-\frac{1}{2}\mu_0 M^2$  are  $\pm 0.02 \times 10^6 \text{ J T}^{-1} \text{ m}^{-3}$  and  $\pm 0.3 \times 10^5 \text{ J m}^{-3}$  respectively. For the Fe/Cu/NiFe samples,  $M$  refers to the magnetic bilayers.

Sample	$M$ ( $10^6 \text{ J T}^{-1} \text{ m}^{-3}$ )	$-\frac{1}{2}\mu_0 M^2$ ( $10^5 \text{ J m}^{-3}$ )	$K$ ( $10^5 \text{ J m}^{-3}$ )
Ni(20 Å)/Fe(20 Å)	1.12	-7.9	-1.7 ± 0.8
Ni(20 Å)/Fe(30 Å)	1.24	-9.7	-2.8 ± 0.6
Ni(20 Å)/Fe(50 Å)	1.38	-12.0	-1.5 ± 0.6
Ni(20 Å)/Fe(80 Å)	1.48	-13.8	-2.2 ± 0.6
Fe(30 Å)/Cu(10 Å)/NiFe(30 Å)	1.04	-6.8	-0.8 ± 0.4
Fe(30 Å)/Cu(20 Å)/NiFe(30 Å)	1.04	-6.8	-0.2 ± 0.4
Fe(30 Å)/Cu(30 Å)/NiFe(30 Å)	1.04	-6.8	-0.4 ± 0.4
Fe(30 Å)/Cu(50 Å)/NiFe(30 Å)	1.04	-6.8	+0.1 ± 0.4

### 3.2. Ni/Fe multilayers—magnetic results

The relative absorption intensities of the outer/middle/inner doublets that constitute a Mössbauer magnetic sextet component are given by the ratio

$$3: \frac{4 \sin^2 \theta}{1 + \cos^2 \theta} : 1$$

where  $\theta$  is the mean angle of the hyperfine-field (atomic magnetic moment) direction to the gamma ray beam. For the spectra of all samples shown in figure 2 the relative areas are 3:4:1 giving  $\theta = 90^\circ$ , representing iron moments lying in plane. In order to measure the anisotropy energy associated with rotating the magnetization of the layers out of plane, external fields were applied normal to the layer plane and the equilibrium orientation of the iron moments measured for each field value from the relative line intensities of the Mössbauer spectrum. The series of spectra for the 20/30 multilayer are shown in figure 3, where the relative line intensity ratio is seen to change from 3:4:1 ( $\theta = 90^\circ$ ) at applied field  $B = 0$  to 3:0:1 ( $\theta = 0^\circ$ ) for  $B = 2.01 \text{ T}$ . In the spectra of figure 3 (and of figure 5—see later) a small singlet peak is observed at  $\sim 0.2 \text{ mm s}^{-1}$ . This arises from absorption in the window of the magnet cryostat and is not present in the spectra of figure 2 which were taken on a room temperature spectrometer.

The dependence of the magnetic energy  $W$  of the system in an applied field  $B$  on the angle  $\theta$  can be written as

$$W = K \sin^2 \theta - \frac{1}{2}\mu_0 M^2 \sin^2 \theta - MB \cos \theta$$

where the first term represents the intrinsic anisotropy energy of the multilayers—composed of crystalline volume and interface anisotropies, the second term is the magnetostatic demagnetizing energy and the third term is the applied-field energy. For the intrinsic anisotropy term  $K$ , positive values favour out-of-plane orientation of moments and negative values favour in-plane alignment.

This dependence gives rise to the expression

$$\cos \theta = \frac{MB}{\mu_0 M^2 - 2K}$$

relating the equilibrium orientation of the moment  $\theta$  to the value of the applied field  $B$ . The experimental points for the variation of  $\cos \theta$  with  $B$  taken from the spectra of figure 3 are shown in figure 4. The slopes of these graphs combined with the magnetization  $M$  measured

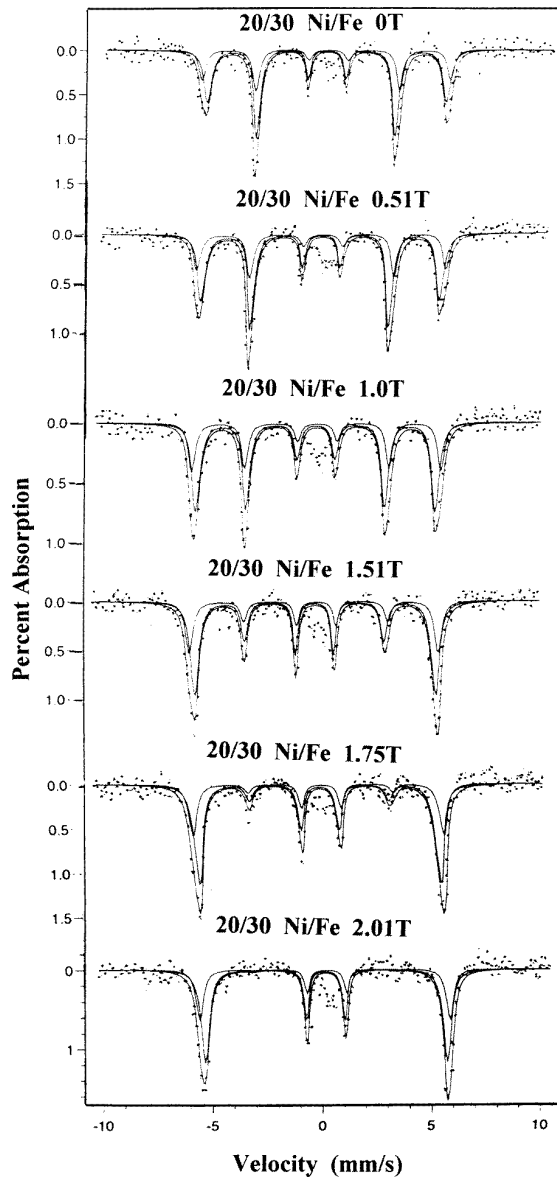


**Figure 3.** Mössbauer spectra of the Ni/Fe 20/30 multilayer sample at 4.2 K with increasing values of external field applied normal to the layers. The spectra are fitted with magnetic sextet components each corresponding to a distinct iron-atom environment. In each spectrum the individual components are shown in addition to the overall summed fit. As the applied field increases it is seen that, for each sextet component, lines 2 and 5 (counted from the left) decrease in intensity corresponding to a decrease in  $\theta$ —the angle between the magnetic moments and the field direction.

for each multilayer and listed in table 2 enabled the values of the magnetic anisotropy energy  $K$  to be evaluated. The values are listed in table 2. The negative sign for  $K$ , seen for all of the Ni/Fe systems, represents a preference for in-plane orientation. This negative intrinsic anisotropy  $K$  adds to the (larger) values of demagnetizing energy listed in table 2 to give the



### Ni/Fe 2030 Multilayer

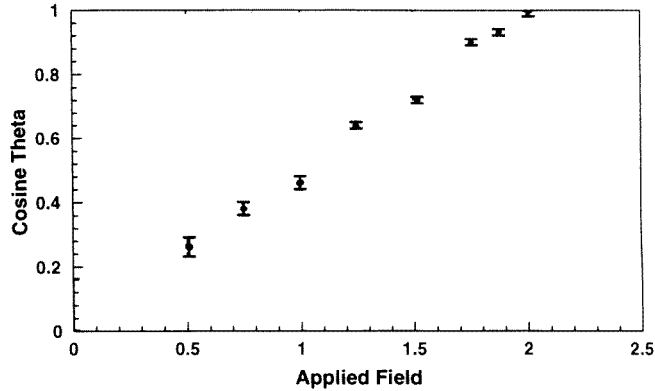


**Figure 4.** A graph of  $\cos\theta$  versus applied field  $B$  for the spectra shown in figure 3 taken for the Ni/Fe 20/30 multilayer.

total anisotropy energy favouring in-plane orientation of magnetic moments. Analysis of the intrinsic anisotropy energies into volume and interface contributions is treated in the discussion section.

### 3.3. Fe/Cu/NiFe multilayers—characterization

The series of multilayers  $[\text{Fe}(30 \text{ \AA})/\text{Cu}(x \text{ \AA})/\text{NiFe}(30 \text{ \AA})]_{50}$ , with  $x = 10 \text{ \AA}$ ,  $20 \text{ \AA}$ ,  $30 \text{ \AA}$  and  $50 \text{ \AA}$ , were characterized in a similar manner to the Ni/Fe multilayers. Transmission electron microscopy showed layering on microtomed cross section slices consistent with layer thicknesses evaluated from calibrated deposition rates. Electron diffraction on the JEOL 3010 showed ring patterns with identifiable rings corresponding to bcc iron, fcc copper and fcc NiFe with a lattice constant  $a = 3.52 \text{ \AA}$  consistent with the alloy composition 80% Ni and 20% Fe.

Mössbauer spectra of the 30/10/30 sample taken at 4.2 K are shown in figure 5. The spectra are fitted with two sextet components; the more intense component has an isomer shift of  $\delta = 0.13 \pm 0.01 \text{ mm s}^{-1}$ , a quadrupole interaction of  $-0.02 \pm 0.01$  and a hyperfine field  $B_{hf} = 340 \pm 2 \text{ kG}$  which is characteristic of bcc iron at 4.2 K. The less intense sextet has isomer shift  $\delta = 0.14 \pm 0.02 \text{ mm s}^{-1}$ , a quadrupole interaction of  $0.00 \pm 0.02$  and hyperfine field  $B_{hf} = 301 \pm 4 \text{ kG}$  characteristic of a Ni(80%)Fe(20%) alloy with fcc structure. The relative absorption intensities are in the ratio 80:20 as expected for layers of equal thickness. It thus seems straightforward to identify the observed components with layers of bcc iron and fcc NiFe alloy. The consistency of the absorption ratios with layers of pure iron and 80% Ni 20% Fe alloy leave no absorption intensity at  $\sim 300 \text{ kG}$  for Fe/Cu interface environment sites.

Magnetization measurements and hysteresis cycles taken with the vibrating-sample magnetometer indicated ferromagnetic coupling between Fe and NiFe layers in all samples. This is confirmed by a corresponding reduction in the effective field  $B_{eff} = B_{hf} + B$  of the Mössbauer spectra of figure 5 as the applied field  $B$  is increased. This is caused by the aligning of the Fe moments in both layers with the field. The opposed directions of the hyperfine field and the magnetic moments of the iron atoms result in partial cancellation of  $B_{hf}$  and  $B$ , reducing  $B_{eff}$  in both components as the applied field is increased.

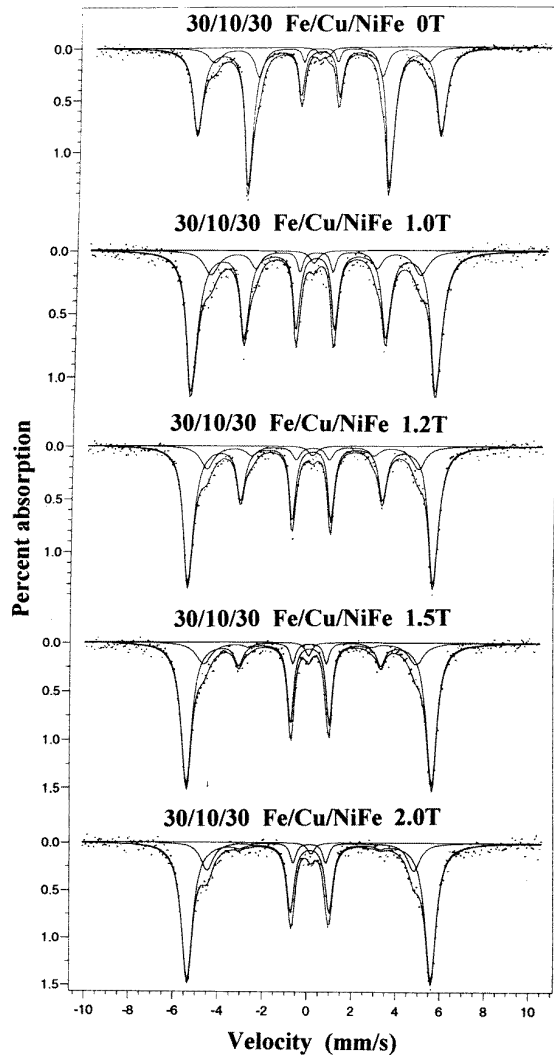


**Figure 5.** Mössbauer spectra of the Fe/Cu/NiFe, 30/10/30 multilayer sample taken at 4.2 K for increasing values of the field applied normal to the layers. The spectra are fitted with magnetic sextet components each corresponding to a distinct iron-atom environment. In each spectrum the individual components are shown in addition to the overall summed fit. The series of spectra show the reorientation of the moments toward the field direction as the field values increase. The decrease in total effective field for both Fe and NiFe components at the larger fields indicates that the moments of these layers are parallel.

#### 3.4. Fe/Cu/NiFe multilayers—results

Series of applied-field Mössbauer spectra such as that shown for the 30/10/30 sample in figure 5 were analysed to give values of the intrinsic anisotropy  $K$ . The quantity of interest is the value of  $K$  for the Fe/NiFe magnetic bilayer between non-magnetic copper layers; thus the appropriate value of the magnetization  $M$  is that of the magnetic bilayer rather than the measured  $M$  that is 'diluted' by the volume of the copper layers. The value of  $M$  for the magnetic bilayers was obtained by extrapolating the linear graph of measured  $M_m$  versus

copper layer thickness back to zero thickness of copper. The bilayer magnetization thus obtained,  $M = (1.04 \pm 0.06) \times 10^5 \text{ J T}^{-1} \text{ m}^{-3}$ , agreed with the value of  $1.10 \times 10^5 \text{ J T}^{-1} \text{ m}^{-3}$  from bulk values for bcc iron and the NiFe alloy. Using this extrapolated value for  $M$  and the slopes of the graphs of  $\cos \theta$  versus  $B$ , values of the intrinsic anisotropy energy  $K$  for the Fe/NiFe bilayers were evaluated and these are listed in table 2.

## 4. Discussion

### 4.1. Ni/Fe multilayers

The anisotropy energy of a magnetic layer is conventionally split into a component  $K_V$  dependent on the bulk anisotropies and a component  $K_S$  dependent on the anisotropy arising from interface interactions [3]. In this analysis the demagnetizing energy  $-\frac{1}{2}\mu_0 M^2$  appears explicitly separately from  $K_V$ —in some other studies it is included in the volume component of the anisotropy. The values of the demagnetizing energy  $-\frac{1}{2}\mu_0 M^2$  listed in table 2 are seen to be nearly an order of magnitude greater than the measured values of the intrinsic magnetic anisotropies  $K$ . Thus the demagnetizing term is the dominating effect in determining the in-plane moment orientation but it is in the values of the intrinsic anisotropy energy  $K$  that the contributions to the anisotropy energy from atomic interactions in the bulk,  $K_V$ , and at the interfaces,  $K_S$ , occur. Measurements of  $K$  on a series of multilayers with different layer repeat distances allow evaluation of  $K_V$  and  $K_S$ , which can be related to the measured intrinsic anisotropy  $K$  by

$$K = K_V + \frac{2K_S}{\Lambda}$$

where  $\Lambda$  is the layer repeat thickness and the factor 2 appears to represent there being two interfaces per layer. The variation of measured values of  $K$  versus  $1/\Lambda$  is shown in figure 6. The fitted line gives values of  $K_V = (-5 \pm 1) \times 10^4 \text{ J m}^{-3}$  and  $K_S = (-0.6 \pm 0.4) \times 10^{-3} \text{ J m}^{-2}$ . This value of  $K_V$  is comparable with the magnetocrystalline bulk anisotropy energy for bcc

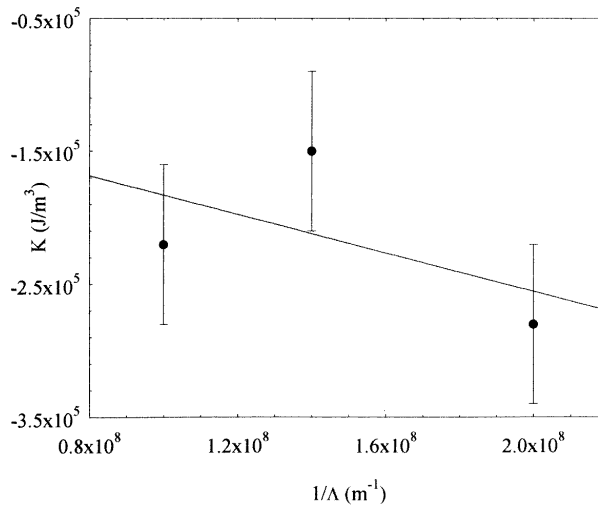


**Figure 6.** Variation of the intrinsic anisotropy energy  $K$  with  $1/\Lambda$  for Ni/Fe multilayers where  $\Lambda$  is the layer repeat distance. The values of  $K_S$  and  $K_V$  are obtained from the slope and intercept on the  $K$ -axis respectively.

iron ( $4.1 \times 10^4 \text{ J m}^{-3}$ ) and favours in-plane moment orientation. The value of  $K_S$  for Fe(bcc)/Ni(fcc) interfaces has not, to our knowledge, been reported in the literature but is in line with determinations of interface energies of Ni/Cu and Ni/Au layer systems where the values have similar magnitude and favour in-plane moment orientation [5]. In plotting figure 6 the point for the 20/20 multilayer was omitted, since the characterization studies showed that the interface may not be the same as in the other samples where the structures were shown unambiguously to be bcc iron and fcc nickel. Theoretical calculation of  $K$ -values has proved difficult. A first-principles calculation of  $K$  for an fcc Co(1 ML)/Ni(2 ML) system predicted normal anisotropy in agreement with experiment [18], but calculations have not been made for Ni/Fe systems. A simple band picture considering hybridization effects [19] predicts in-plane anisotropy for Ni/Cu and out-of-plane anisotropy for Fe/Cu layer systems in agreement with most observed values [5], but no prediction was made for Ni/Fe systems.

#### 4.2. Fe/Cu/NiFe multilayers

In the series of Fe/Cu/NiFe multilayer samples, the Fe/NiFe bilayers are the same throughout the series—the variation arising only from the thickness of the non-magnetic copper layer that separates them. In this series the values of  $K_V$  and  $K_S$  that constitute the intrinsic anisotropy energy of the magnetic bilayer bounded by copper layers should be the same for each sample. The variation between samples may depend on the strength of the magnetic coupling between bilayers—this is reduced as the thickness of the intervening copper layer increases. A graph of measured intrinsic anisotropy  $K$  versus copper layer thickness is shown in figure 7. There appears to be some evidence for the alignment of moments in plane to be progressively preferred as the thickness of the copper layer is reduced. Such a trend is barely significant given the errors on the individual points, but gives rise to interesting speculations about possible mechanisms for such behaviour. At large values of copper layer thickness the magnetic bilayers will be decoupled and for this case the magnetic anisotropy energy depends only on the intrinsic bulk and interface energies. A given bilayer contains Cu/Fe, Fe/NiFe

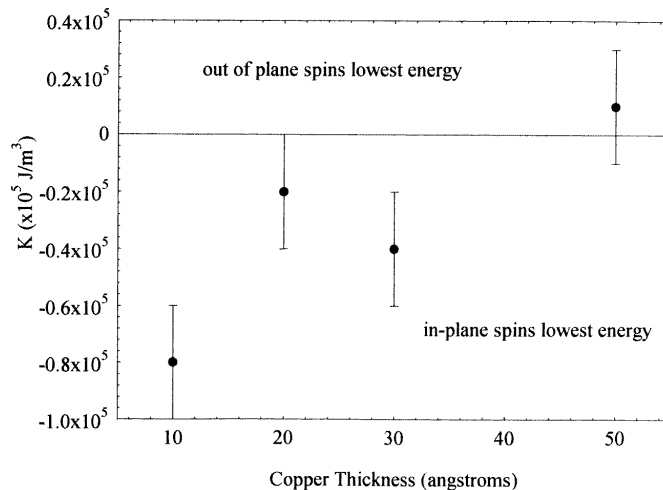


**Figure 7.** Variation of the intrinsic anisotropy energy  $K$  with thickness of the non-magnetic layer in a Fe/Cu/NiFe series of multilayers. The trend in  $K$  is toward increasing in-plane moment alignment as the copper layer thickness is decreased.

and NiFe/Cu interfaces. Assuming a mean value of  $K_S = -0.2 \times 10^{-3} \text{ J m}^{-2}$  for the Ni/Cu interface from the collected data [5] and the measured value  $K_S = (-0.6 \pm 0.4) \times 10^{-3} \text{ J m}^{-2}$  for the Ni/Fe interface, a positive  $K_S$ -value is required for the Fe/Cu interface to give rise to the positive  $K$ -value measured for the 30/50/30 multilayer and shown in figure 7. Collected values from the literature [5] confirm the out-of-plane anisotropy for the Fe/Cu interface. The apparent trend in figure 7 shows an increase in in-plane anisotropy as the copper layer thickness is decreased and the interaction between magnetic bilayers increases.

Possible interlayer interactions that can give rise to anisotropy energy are (i) dipole–dipole interaction between layers and (ii) anisotropy exchange (Dzyaloshinsky–Moriya interaction) between layers. The dipole–dipole interaction between ferromagnetically coupled bilayers favours out-of-plane anisotropy. This interaction predicts the opposite of the trend seen in figure 7 and is thus not the dominant mechanism. The Dzyaloshinsky–Moriya interaction energy  $E_{\text{DM}}$  is of the form

$$E_{\text{DM}} = \mathbf{L} \cdot \mathbf{M}_1 \times \mathbf{M}_2$$

where  $\mathbf{M}_1$  and  $\mathbf{M}_2$  are the magnetizations of adjacent bilayers and  $\mathbf{L}$  is an exchange constant. For such a mechanism to cause the observed trend requires some canting between  $\mathbf{M}_1$  and  $\mathbf{M}_2$ —the in-plane magnetizations of adjacent levels—and a negative magnitude for  $\mathbf{L}$  which must be aligned normal to the layers. While this mechanism is not proved to operate, such a possibility remains an interesting speculation.

### Acknowledgments

The work was funded by an EPSRC grant. J A Hutchings and K Newstead were supported by EPSRC research studentships.

### References

- [1] Falicov L M, Pierce D T, Bader S D, Gronsky R, Hathaway K B, Hopster H J, Lambert D N, Parkin S S P, Prinz G, Salamon M, Schuller I K and Victoria R H 1990 *J. Mater. Res.* **5** 1299–340
- [2] Gradmann U 1993 *Handbook of Magnetic Materials* vol 7, ed K H J Buschow (Amsterdam: Elsevier) pp 1–95
- [3] Bland J A C and Heinrich B (ed) 1994 *Ultrathin Magnetic Structures* vols I, II (Berlin: Springer)
- [4] den Broeder F J A, Hoving W and Bloemen P J H 1991 *J. Magn. Magn. Mater.* **93** 562–70
- [5] Johnson M T, Bloemen P J H, den Broeder F J A and de Vries J J 1996 *Rep. Prog. Phys.* **59** 15 409–58
- [6] Heinrich B and Cochran J F 1993 *Adv. Phys.* **42** 523–639
- [7] Li Y, Polaczyk C, Klose F, Kapoor J, Maletta H, Mezei F and Riegel D 1996 *Phys. Rev. B* **53** 5541–6
- [8] Kuch W and Parkin S S P 1998 *J. Magn. Magn. Mater.* **184** 127–36
- [9] Krishnan R, Gupta H O, Lassri H, Sella C and Kaabouchi M 1991 *J. Appl. Phys.* **70** 6421–3
- [10] Johnson C E, Ridout M S, Cranshaw T E and Madsen P E 1961 *Phys. Rev. Lett.* **6** 450–1
- [11] Korecki J and Gradmann U 1985 *Phys. Rev. Lett.* **55** 2491–4
- [12] Jennet N M and Dingley D J 1991 *J. Magn. Magn. Mater.* **93** 472–6
- [13] Colombo E, Fratucello G and Ronconi F 1987 *J. Magn. Magn. Mater.* **66** 331–6
- [14] Colombo E, Donzelli O, Fratucello G B and Ronconi F 1991 *J. Magn. Magn. Mater.* **93** 597–600
- [15] Fratucello G B, Colombo E, Donzelli O and Ronconi F 1989 *Hyperfine Interact.* **45** 255–62
- [16] Edelstein A S, Kim C, Quadri S B, Kim K H, Browning V, Yu H Y, Maruyama B and Everett R K 1990 *Solid State Commun.* **76** 1379–82
- [17] Ellerbrock R D, Fuest A, Schatz A, Kenna W and Brand R 1995 *Phys. Rev. Lett.* **74** 3053–6
- [18] Daalderop G H O, Kelly P J and den Broeder F J A 1992 *Phys. Rev. Lett.* **68** 682–5
- [19] Givord D, McGrath O F K, Meyer C and Rothman J 1996 *J. Magn. Magn. Mater.* **157–8** 245–9